Int. J. Electrochem. Sci., 7 **(2012)** 1443 - 1458

International Journal of
ELECTROCHEMICAL
SCIENCE
www.electrochemsci.org

Corrosion Behaviour of Amorphous Niobium Oxide Coatings

P. N. Rojas, S. E. Rodil

Instituto de Investigaciones en Materiales, Universidad Nacional Autónoma de México, Ciudad Universitaria, México D. F.
*E-mail: nayuritkd@gmail.com

Received: 21 September 2011 / *Accepted:* 14 January 2012 / *Published:* 1 February 2012

Niobium oxide films were evaluated as possible candidates for corrosion resistant biomedical coatings using electrochemical methods. The films were deposited on medical grade stainless steel using a reactive magnetron sputtering system starting from a pure Nb target. The long-term stability of the films was evaluated by electrochemical impedance spectroscopy (EIS) as a function of time up to 500 hrs using two different simulated body fluids. The results indicated that the electrochemical stability of the coatings is highly dependent upon the chemical composition of the solution. In 0.89% NaCl, the coating failed by delamination, while in the Hartman solution, the niobium oxide film was very stable providing protection to the stainless steel substrate.

Keywords: Corrosion; Impedance Spectroscopy; Niobium oxide; Thin Films

1. INTRODUCTION

Several metallic alloys fulfill the mechanical requirements of orthopedic prosthesis and fixation devices. However, only few of them offer the required biocompatibility and corrosion resistance in the physiological medium, as for example Co–Cr alloys, titanium alloys or certain stainless steels[1]. The AISI 316L stainless steel is often used for temporary devices in orthopedic surgery such as plates, nails, etc due to their lower cost and availability. However, it is well known that the presence of Cl^- ions in human body stimulates pitting and crevice corrosion attack [2], especially dangerous for stainless steel. It corrodes in the body environment and release iron, chromium and nickel ions and these ions are found to be powerful allergens and carcinogens [3]. In order to solve the problems associated to these localized corrosion attacks and leaching of metallic ions, it is necessary to improve the corrosion resistance of currently used type 316L SS. Different alternatives to improve the corrosion response of stainless steel have been proposed, where surface modifications is one of the most promising [4,5].

Surface modification for corrosion and oxidation protection can be achieved by physical vapor deposition (PVD) of ceramic coatings on the steel and, different functional and protective coatings have been developed so far [6]. Particularly interesting are those based on transition metal ceramics; nitrides and oxides, due to their enhanced surface hardness and wear resistance. In this work, we evaluate the corrosion resistance of amorphous niobium oxide films using two different electrolytes that simulates body fluid conditions.

The biocompatibility of niobium oxide films prepared by different techniques has been previously evaluated [7]. In all cases, the biological results suggested that the material is a potential candidate for surface modification of metallic implants and it would be more attractive if the film provides both corrosion resistance and biocompatibility.

The amorphous niobium oxide films were deposited by magnetron sputtering on AISI 316L steel. The corrosion resistance was evaluated in solutions simulating the mineral concentration of body fluids; 0.89 wt% NaCl and Hartman solution. The latter contains, apart from similar Na and Cl ionic concentrations, an organic molecule; the lactic acid.

The Hartman solution is a medical liquid used to replace body fluid and mineral salts, it is isotonic with blood and thus will give us information about the corrosion response of the samples in an electrolyte that simulates the mineral concentration of the physiological fluids. Basically, it contains sodium (131 mEq), chloride (111 mEq), potassium (5 mEq) and calcium (4 mEq) ions plus lactic acid. Lactic acid (2-hydroxypropanoic acid) is a chemical compound involved in a variety of biochemical processes. In solution, the lactic acid can lose a proton from the acidic groups producing the lactate ion ($CH_3CH(OH)COO$). The blood lactate concentration in humans changes from 1-2 mmol/L at rest, to 20 mmol/L during extreme exercise. The lactate concentration in Hartman solution is slightly higher, 29 mmol/L, but very similar to the concentration of lactated Ringer´s solution, another solution commonly used to simulate corrosion processes in physiological fluids. The use of a solution containing an organic acid also allows us to elucidate the effect of the adsorption of the organic molecule on the corrosion phenomena. In order to simulate the in vivo conditions, we should use electrolytes containing proteins. However, the proteins are highly complex organic molecules compared to the low molecular weight lactic acid and their adsorption mechanisms depend on too many external factors. Therefore, as an initial stage of the research where the purpose is to evaluate the material (amorphous niobium oxide films), a more simple and well-controlled electrolyte containing organic molecules was chosen to study the electrochemical response in electrolytes containing salt concentrations similar to body fluids and at least one organic component. Qualitatively, the adsorption process of the organic molecule on the surfaces was evaluated by ellipsometry kinetic spectra.

2. EXPERIMENTAL DETAILS

2.1 Materials

Pieces of medical grade stainless steel (AISI316L) with dimensions of 10 x 10 x 1 mm^3 were used as the substrate material for the electrochemical studies. The surface was prepared with SiC grits up to 600grade and then cleaned using an ultrasonic bath during 15 minutes using consecutively

acetone, ethanol and deionized water. The nominal composition of the stainless steel (SS) substrates was given by the steel-company (Tyysenkrup Mexinox) as 0.0019%C, 0.22%Si, 1.38%Mn, 17.21%Cr, 10.60%Ni, 2.05%Mo, 0.004%Ti, 0.043%N, 0.31%Cu, 0.085Co, 0.026%P, 0.026%S, balance Fe.

Pure Nb metal (99.9%) was used as the target material in a reactive magnetron-sputtering deposition system. The deposition conditions for the electrochemical evaluation were chosen previously, as reported in another paper [8]. Briefly, the pressure and Ar/O_2flow ratios were varied, while the other deposition conditions were fixed. The whole set of samples were tested by potentiodynamic polarization and polarization resistance. Analyzing these data and using as criteria lower corrosion current densities and larger polarization resistances, the best deposition conditions were selected. Using these conditions, a set of about 30 samples (150 nm thick) were deposited for further electrochemical tests. In the present paper, the electrochemical characterization using electrochemical impedance spectroscopy (EIS) after long-term immersion periods is presented. There is very few information concerning the electrochemical response of Nb-based thin films and none concerning its evaluation using electrolytes that simulate physiological fluids.

The deposition conditions and some evaluated film properties are shown in table 1. It is interesting to see that the refractive index of the films was very close to the values for a crystalline Nb_2O_5 suggesting that the amorphous oxide layer was relatively dense. The composition of the films was close to Nb_20_5, and the X-ray diffraction experiments demonstrated that they were amorphous [8], we labeled the samples as *a*-Nb_2O_5, where the *a* comes from the amorphous character of the films.

Table 1. Deposition conditions chosen from a previous optimization experiment and film properties as reported in [9].

Deposition Conditions and Film Properties	
Pressure (Pa)	3
O_2/Ar flow	0.3
dc-Power (W)	80
Target-substrate (mm)	50
Thickness (nm)	150
Nb/O (at%.)	0.418
Hardness (GPa)	4.5 ± 0.8
Elastic Modulus (Gpa)	119.3
Band gap Eg (eV)	3.4
Refractive index at 2.25 eV	2.25

2.2 Corrosion testing

The investigation of the electrochemical behavior of the amorphous niobium oxide films was carried out in both 0.89 wt% NaCl and Hartman solutions open to air, not stirred and at room temperature (20ºC - 24ºC, maximum variation measured during the experiments). The Hartman

solution was obtained from Abbott Laboratories de Mexico SA de CV and its composition is shown in table 2. The experimental set up consisted of a three electrode cell (saturated calomel electrode, SCE as reference and platinum as counter-electrode), in which test specimens were placed in a flat-cell configuration, where only 0.1 cm^2 of the coated substrate face was exposed to the electrolyte. All measurements were carried out with the cell inside a Faraday cage. Potentiodynamic and electrochemical impedance spectroscopy measurements were obtained using a PCI400 Gamry potentiostat and analysis of the electrochemical data was done using the Echem Analyst software. The electrochemical evaluation was done as a function of the immersion time using impedance spectroscopy in order to evaluate the long-term performance of the coatings.

Table 2. Electrolytes composition in g/L.

COMPONENT (g/L)	Sodium chloride solution	Hartmann Abbott solution
$CaCl_2$		0.20
KCl		0.30
NaCl	8.9	6.0
Sodium lactate		3.1

The experimental procedure consists of:

1. Acquisition of the open circuit potential (OCP) vs. time: In this case, the samples were kept in the solution for 9500s without polarization while the OCP was recorded.
2. Using the same sample as above and after the 9500 s, where a steady state was reached, potentiodynamic polarization (PP) curves were obtained using a scan rate of 0.166 mV/s and from -100 mV to +250 mV relative to the OCP.
3. Since the PP measurements could affect the sample properties, a new sample (which was deposited at the same time) was used to obtain the EIS spectra. In this case, the samples were kept in the solution for 9500s without polarization to reach steady state. Then, the impedance spectra were recorded at the final OCP in the 10 mHz-10 KHz frequency range, with a data density of five frequency points per decade. The applied alternating voltage has amplitude of 10 mV (rms). The sample was then kept in the solution and collection of EIS spectra for each system was conducted at regular intervals up to 500 h of immersion.

2.3 Analysis of the impedance spectra

After each experiment, the AC impedance was displayed as Bode plot; log |Z| versus log f, and θ versus log f, where |Z| is the absolute value of the impedance, θ is the phase angle and f is the frequency in Hz. Stainless steel and PVD coated steels exposed to an aqueous solution have been investigated by several researchers [5,9,10]. The analysis of the impedance spectra has been made using equivalent electronic circuits (EC) as shown in Fig. 1. The electrochemical response of PVD

coatings have been studied by different research groups showing that there is a characteristic response, which is a consequence of the films nano or micro porosity, as schematically depicted in Fig. 1a, where the steel substrate is exposed to the electrolyte through permeable defects (e.g. pores). The electrochemical response for a material having these characteristics can be modeled using parallel-connected elements (R_{pore}; C_c)-(R_s; C_s) as shown in Fig. 1b. The (R_{pore}; C_c) represents the coating and (R_s; C_s) are the polarization resistance and capacitance of the double layer at the steel substrate, respectively.

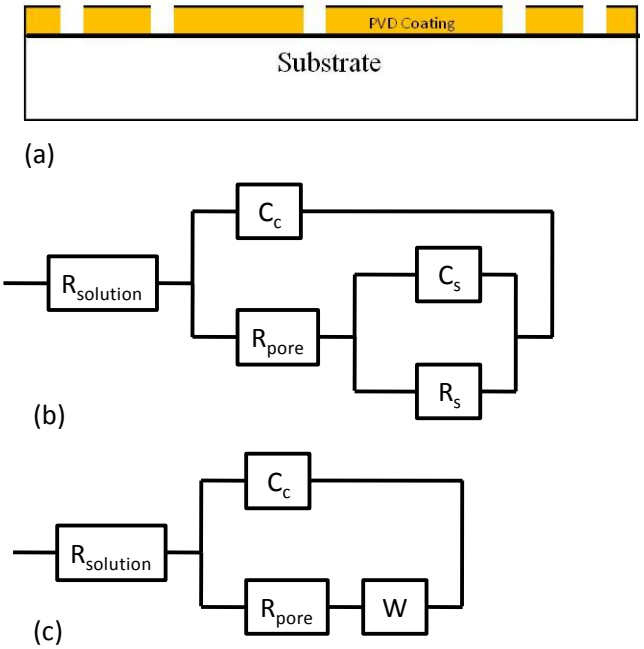

Figure 1. Electrical equivalent circuits used to fit the impedance spectra and graphical representation of the coating porosity as paths where the electrolyte can reach the substrate. (a) Film porosity sketch, (b) Circuit used for the SS substrate and (c) circuit used for the coating/SS system.

The substrate is reached through the sample-porosity leading to an electrical charge transfer at the substrate/coating interface, (R_s; C_s). Indeed, the capacitances are usually substituted by constant phase elements (CPE) to take into account the non-homogeneity of the surfaces. A similar circuit has been used to model the stainless steel response, where the (R_{pore}; C_c) represents the dense-high dielectric passive film existing in stainless steel. This circuit is characteristic of EIS spectra showing two time constants observed as two minima in the Bode-phase spectra, or two semicircles in the Nyquist (real versus imaginary part of the impedance). However, Liu et. al. [9,11] have shown that for ceramic films deposited on stainless steel, these two minima are sometimes no distinguishable. Thus, in such cases, it is better to use a simplified circuit (see figure 1c), where only one (R, C_{c+f}) circuit is considered and the c+f subscript refers to the combined response of the PVD-coating plus the steel passive film. The Warburg impedance included in circuit 1c takes into account diffusion processes that might constraint the ionic conductivity, affecting the electrochemical current density. Obviously, this

limited diffusion, which occurs through the coating defects, is strongly correlated to the film microstructure. Thus, the use of the Warburg impedance as part of the electronic circuit depends on the film's response.

For this work, the substrates (AISI316L) were modeled using the circuit in figure 1b and the *a*-Nb_2O_5 coatings deposited on stainless steel were modeled using the circuit in figure 1c, including the Warburg impedance, as explained in more detail later.

2.4 Adsorption kinetics

Ellipsometry was used as a technique to monitor in time the adsorption of the organic molecules (lactic acid) on both surfaces. For these kinetic spectra, a phase modulated ellipsometer (HORIBA-JobinYvon UVISEL) was used. Ellipsometry is a sensitive optical technique that measures the change in the state of the polarization of light upon reflection from a planar interface in order to gain information about the structure of that interface. The technique has matured over the last four decades owing to a combination of instrumental developments such as laser sources and phase-modulated polarizers and advances in data analysis derived from theoretical insights and faster computers. In any ellipsometry experiment, upon reflection of the polarized light at a known angle-of-incidence and with a known wavelength λ, the relative change in the amplitude of the polarized light (expressed as Ψ) and the relative change in the phase difference between the parallel and perpendicular components of the light (expressed as Δ) are determined.

These angle parameters are extremely sensible to any variation in the surface (changes of the order of 0.001° are detectable), including an adsorbed layer of organic molecules due to the different refractive index and the thickness of the adsorbed layer. Ellipsometry have been used to perform adsorption experiments in situ and real time demonstrating being a precise analysis of adsorption kinetic [12] . In this work, we measured the kinetic adsorption spectra using ellipsometry to qualitatively confirm the adsorption of the organic molecule (lactic acid) on the surfaces and if the differences in such adsorption could be correlated to the electrochemical response.

3. RESULTS

3.1 Open Circuit Potential (OCP)

Figure 2 shows the continuous variation of the open circuit potential during the first 2.5 hours of immersion. It might be observed that there are large differences in the response of the same material to the different electrolytes, even though the Cl^- ionic concentration is similar for both electrolytes. The most noble and stable potential was obtained for the coating in the Hartman solution (-0.05V), reaching a fairly steady value after few minutes of immersion. This is not the case for the coating in the NaCl solution, where a fast decreased in the potential was observed during the initial minutes of the test, which suggested film breakdown.

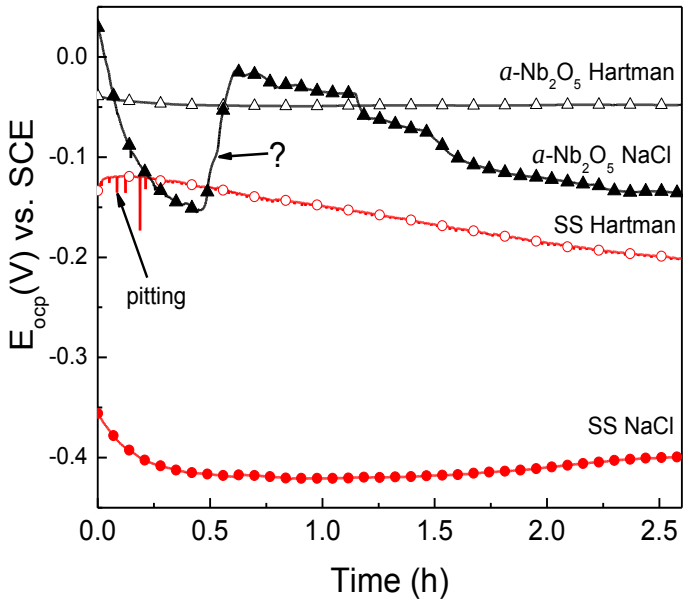

Figure 2. OCP as a function of the immersion time for the SS and the *a*-Nb_2O_5 coating in the two solutions; closed symbols correspond to the Hartman solution, open symbols to NaCl solution.

The latter increase in the potential is not clear, but it is unlikely that re-passivation has occurred in such a short time and moreover the following decrease confirms the film failure. For the SS substrate, the potential is more positive in Hartman (-0.2 V) than in NaCl (-0.4V), however there is a continuous decrease with time without stabilization and some indications of local pitting corrosion were observed at the initial minutes.

3.2 Potentiodynamic Polarization

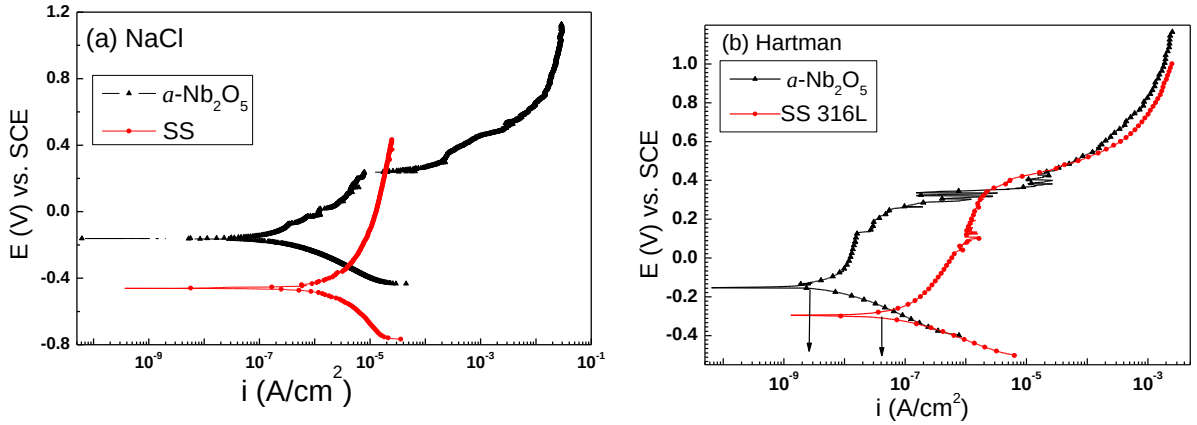

Figure 3. (a) Potentiodynamic polarization curves for SS and *a*-Nb_2O_5 coating after 2.5 hours of immersion in 0.89 wt% NaCl solution. (b) Potentiodynamic polarization curves for SS and *a*-Nb_2O_5 coating after 2.5 hours of immersion in the Hartman solution.

Figures 3 show the polarization curves for both the SS and the coating after 2.5 hrs of immersion in 3(a) NaCl and 3(b) Hartman. The behaviors are not strictly Tafel-like, so no calculations were done. Qualitatively, we can see that in both cases, the corrosion potential is more positive for the coating than for the steel and the approximate corrosion current densities (~I_{corr}) are very low, typical of passive materials (range between 10^{-7}-10^{-9} A/cm^2). The ~I_{corr} (black arrow) is much lower for the coating than for the steel substrate and this difference is larger in the Hartman solution, which is again an indication of the larger corrosion resistance of the coating compared to the SS. However, for the NaCl solution, the film breaks down at a potential (0.23 V) where the SS substrate is still passive, in agreement with the observed failure of the *a*-Nb_2O_5 in NaCl during the OCP experiments.

3.3 Electrochemical Impedance Spectroscopy

The initial EIS spectra (2.5 hours) are shown in Figure 4 using the Bode representation for the SS and the *a*-Nb_2O_5 samples in (a) 0.89 wt% NaCl and (b) Hartman. In both cases, the Bode phase diagram shows a highly capacitive behavior typical of passive materials, supporting the polarization results. The response of the SS is not so different for the two electrolytes, showing a minimum phase angle around -60º at 10 Hz. The impedance spectra of the SS substrate behaved normally and similar to the results reported by other authors [13].

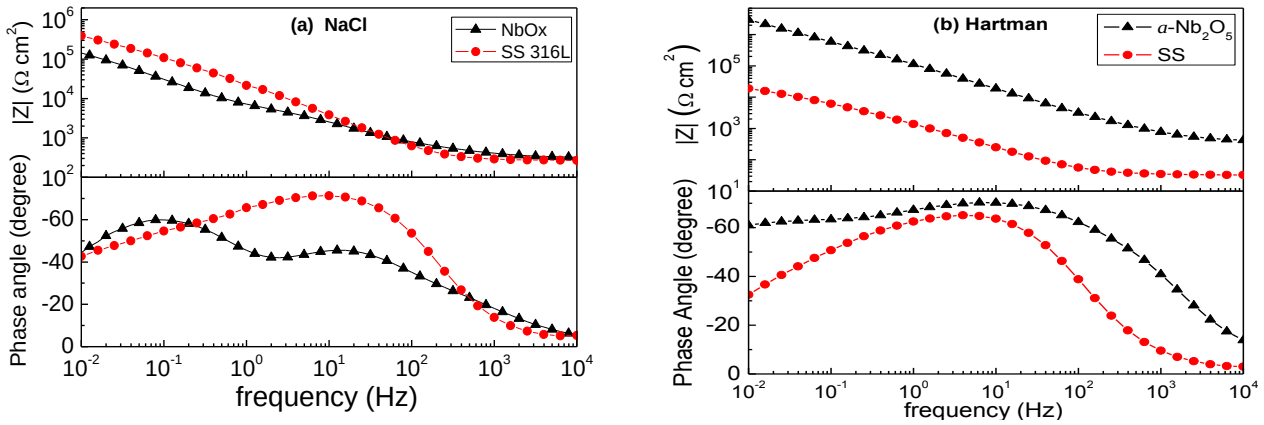

Figure 4. Bode EIS diagrams for SS and *a*-Nb_2O_5 coating after 2.5 hours of immersion in (a) 0.89 wt% NaCl and (b) Hartman solution.

On the other hand, the spectra for the niobium oxide coatings were completely different depending on the electrolyte. In the NaCl (figure 4a), two clear minima can be observed and the phase angle at the 10Hz minima is much lower than in Hartman solution. In Hartman (figure 4b), there is only one broad minima around 10 Hz, reaching about -70°. The minima in these spectra represents the time constants of the (R;C) circuits: the high frequency (~10Hz) minima is associated to the film properties, and the lower frequency minima is associated to the substrate interface, which is reached

through the film porosity. Therefore, the spectra observed in figure 4a for the coating in the NaCl solution indicated that at the initial exposure (2.5 hours) the electrolyte had already penetrated the coating reaching the underlying metal through the porosity. The spectra acquired at longer immersion times, confirmed such penetration and the film-failure was evident by scanning electron microscope (SEM) images obtained after the immersion experiments.

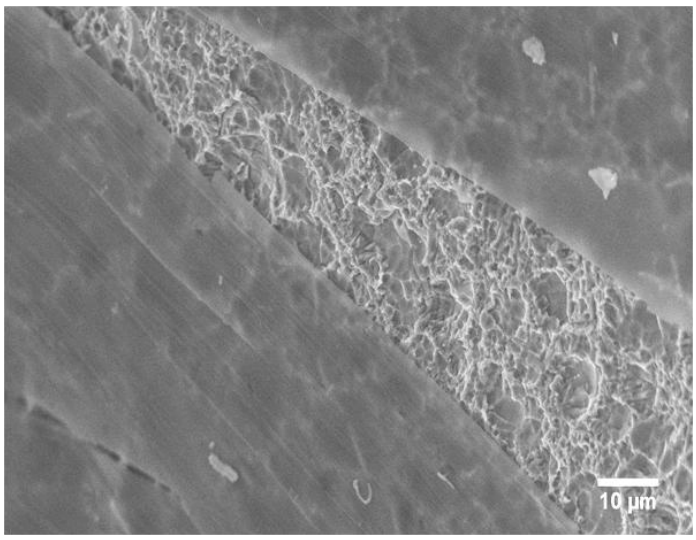

Figure 5. SEM surface micrograph of the *a*-Nb_2O_5 coating after 500 hours of immersion and EIS analysis in 0.89 wt% NaCl solution. The coating delaminated from the substrate and the exposed substrate below is highly corroded, indicating a strong localized corrosion. No delmination or attack was observed for the SS or for both samples when immersed in the Hartman solution.

Figure 5 shows the SEM image of the coating after immersion for 500 hrs in the NaCl solution, where clear delamination areas are observed and a strong chemical attack of the substrate has occurred in such areas. On the other hand, SEM images (not shown) for the a-Nb_2O_5 coating in Hartman solution or the SS in both electrolytes showed no evidence of pitting, localized corrosion or film delamination. Considering the presence of these large areas of delamination and the un-stable behavior of both the OCP and the impedance spectra of the coating when immersed in NaCl, we concluded that the *a*-Nb_2O_5 films immersed in 0.89% NaCl solutions were not stable and break down by adhesive failure. Therefore, no further analyses of the impedance spectra for the samples immersed in NaCl electrolyte were done.

Conversely, the response of the films in the Hartman solution showed a stable behavior and larger impedance values than for the SS. Therefore, the EIS results for the coating and the bare substrates were analyzed on the basis of the equivalent circuits presented in figure 1, which are commonly used for simulation of the coating/substrate systems. Figures 6 show a selection of the impedance spectra obtained for the SS (6a) and the *a*-Nb_2O_5 (6b) samples, as a function of the immersion time, but only for the Hartman solution. In these figures, the experimental data are shown as individual points, while the theoretical spectra obtained from the fits to the relevant equivalent

circuit are shown as lines. The good agreement between experimental and fitted data for both the substrate and coating is clear from the overlapping of dots and lines in both figures (6a and 6b). Before fitting the spectra, the EIS data were validated as conforming to Kramers-Kronig relation obtaining difference errors below 10^{-4} in the complete frequency range.

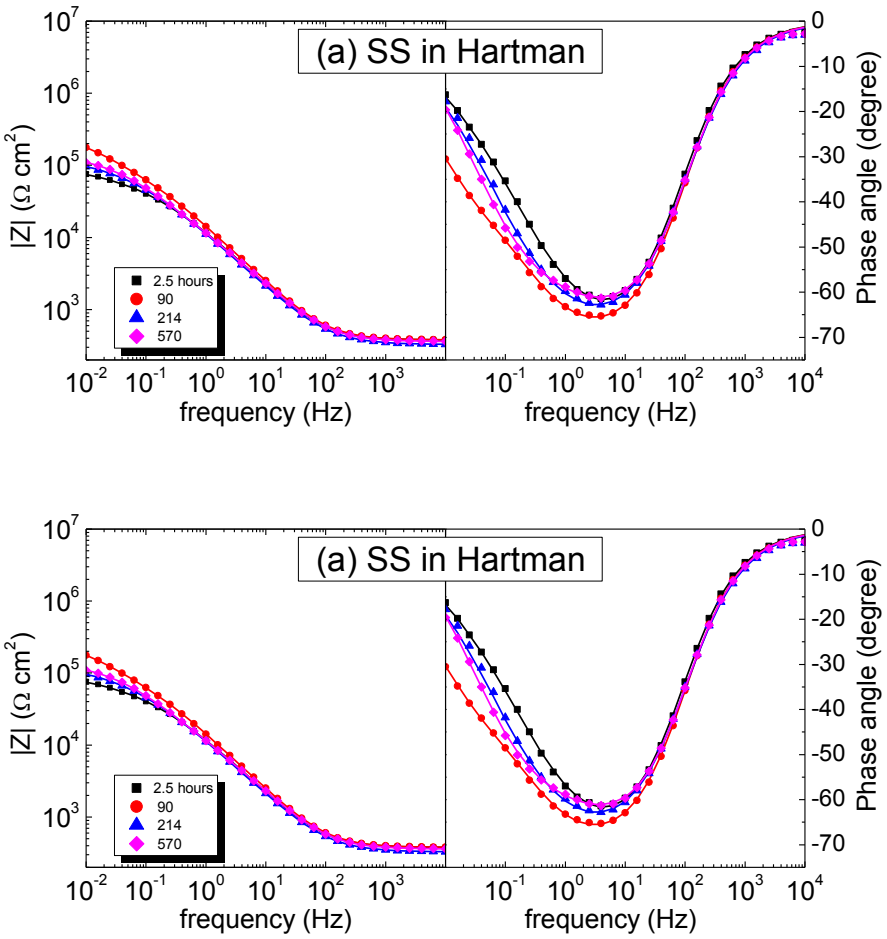

Figure 6. Bode EIS diagrams for (a) SS and (b) *a*-Nb_2O_5 coating as a function of immersion time in the Hartman solution. The corresponding specta for the NaCl solution are not shown since we realized alter than the coating has failed.

The spectra of the SS substrate were modeled using the equivalent circuit shown in figure 1b, which is standard for highly passive stainless steel. Meanwhile, the spectra from the *a*-Nb_2O_5samples on Hartman were modeled using the equivalent circuit shown in figure 1c using the Warburg impedance. The requirement for the Warburg impedance was confirmed by observation of a straight line at the lowest frequencies in the Nyquist representation (Real vs. Imaginary impedance spectra, figure 7) [9,11]. The mathematical results from the fittings of the substrate and the coating in the Hartman solution and as a function of the immersion time are shown in table 3 and 4, respectively.

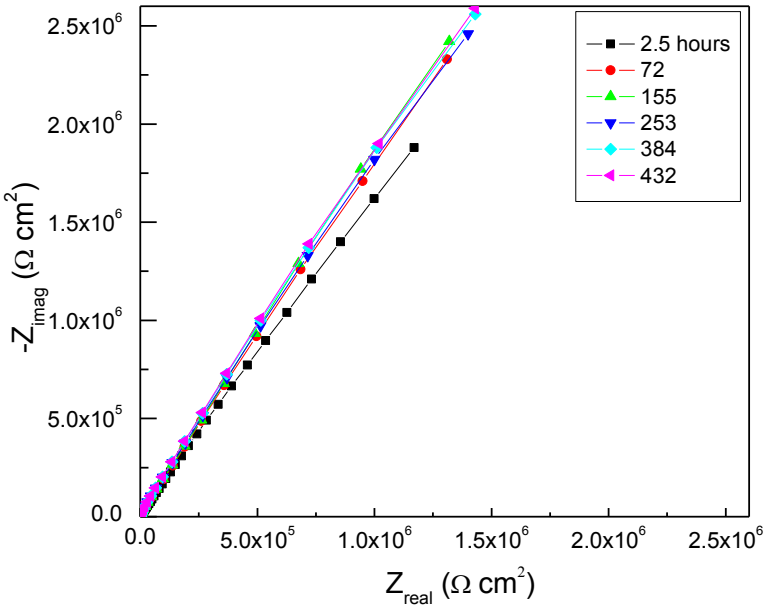

Figure 7. Nyquist diagram for the *a*-Nb_2O_5 coating as a function of immersion time to show the importance of using the Warbug impedance in circuit 1c.

The evolution of the value of the circuit elements with immersion time gives information about the stability of the surfaces. As the two equivalent circuits used to simulate the EIS response of the coating/substrate system and the substrate were different, it is more realistic to analyze the evolution of the polarization resistance (R_p) than that of the individual circuit resistances or capacitances. The polarization resistance is defined as the sum of the resistances in each of the equivalent circuits, which in the case of the coating/substrate system is only ($R_{solution}$+R), while for the substrate is ($R_{solution}$+ R_{pore} + R_s). The evolution of R_p is shown as a function of the immersion time in Figure 8.

Table 3. Electrical components obtained from fitting the circuit in Fig. 1b to the experimental results obtained in electrochemical impedance tests for the stainless steel substrate as a function of the immersion time in Hartman solution. The capacitances in circuit 1b were substituted by CPEs elements, being *n* and *m* the corresponding exponents for the substrate and coating, respectively. The polarization resistance Rp, was calculated as described in section 3.3.

Time (h)	$R_{solution}$(Ω)	R_{pore}(Ω)	CPE_c (S s^m)	m	R_s(Ω)	CPE_s (S s^n)	n	R_p(kΩcm^2)
2.5	375.2	3.55E+04	1.72E-05	0.796	7.19E+04	3.46E-05	0.477	10.78152
74.5	352.3	5.02E+04	4.41E-05	0.762	7.30E+05	9.17E-03	0.305	78.02423
98.5	378.1	8.48E+04	1.50E-05	0.805	2.41E+05	2.16E-05	0.612	32.65781
170.5	357.9	3.77E+04	4.80E-05	0.686	4.83E+04	8.34E-07	0.642	8.63579
218.5	326.6	4.64E+04	1.94E-05	0.783	9.98E+04	2.02E-05	0.404	14.65366
362.5	331.7	7.23E+02	4.90E-05	0.70	2.95E+05	2.73E-05	0.77	29.64542
434.5	326.1	5.42E+04	1.47E-05	0.806	3.52E+05	1.29E-05	0.532	40.60461
578.5	359.2	1.75E+04	1.62E-05	0.800	1.28E+05	1.12E-05	0.562	14.53892

Table 4. Electrical components obtained from fitting the circuit in Fig. 1c to the experimental results obtained in electrochemical impedance tests for the *a*-Nb2O5 coatings as a function of the immersion time in Hartman solution. The capacitance in circuit 1c was substituted by a CPE element, being *n* the corresponding exponent.

Time (h)	$R_{solution}$ (Ω)	CPE_{c+f} (S s^n)	n	W (S $s^{1/2}$)	R (Ω)	R_p (kΩcm^2)
2.5	356.4	2.77E-06	6.75E-01	9.92E-08	6.63E+04	6.66664
74.5	382	2.22E-06	7.46E-01	4.65E-07	1.45E+06	144.9382
170.5	378.2	2.15E-06	7.65E-01	5.31E-07	1.10E+06	110.23782
194.5	371.3	2.15E-06	7.67E-01	5.36E-07	1.12E+06	112.33713
242.5	389.3	2.07E-06	7.74E-01	6.93E-07	1.15E+06	114.93893
290.5	381.9	2.10E-06	7.75E-01	5.52E-07	1.34E+06	133.63819
314.5	386	2.09E-06	7.75E-01	5.04E-07	1.39E+06	139.2386
338.5	371.3	2.15E-06	7.76E-01	5.38E-07	1.30E+06	130.43713
362.5	388.6	2.09E-06	7.77E-01	5.68E-07	1.38E+06	138.23886
410.5	389.8	2.10E-06	7.78E-01	5.12E-07	1.50E+06	150.33898
458.5	391.9	2.10E-06	7.79E-01	4.99E-07	1.57E+06	156.53919
506.5	362	2.15E-06	7.77E-01	4.90E-07	1.72E+06	172.4362

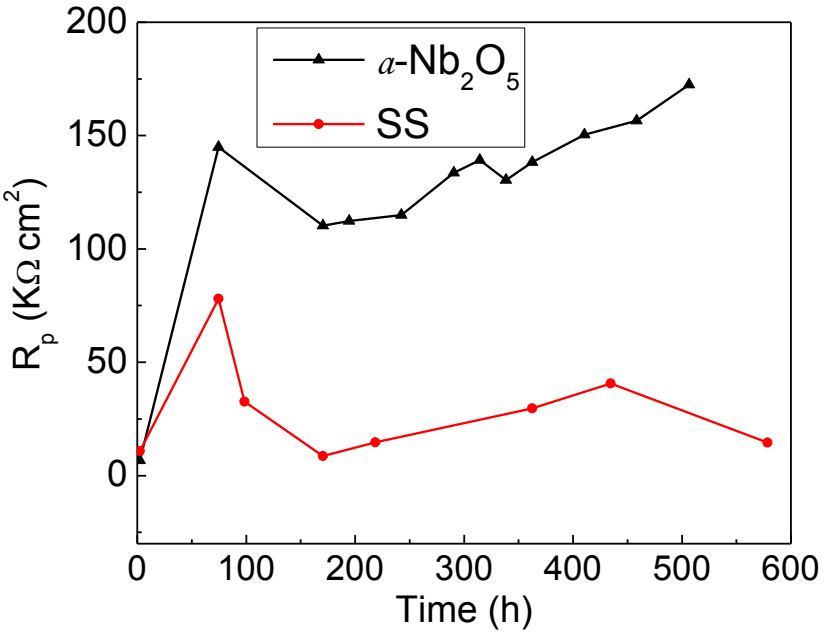

Figure 8. Polarization resistance estimated from the EIS analysis for the SS and *a*-Nb_2O_5 coating as a function of immersion time.The R_p for the coating corresponds to the $R_{solution}$ + R_{c+f} resistance, while for the SS the R_p correspond to the addition of $R_{solution}$ plus R_{pore} and R_s.

The polarization resistance is inversely proportional to the corrosion rate and therefore larger R_p are indicative of lower corrosion rates and thus larger protection. The R_p values are large in both cases, although one order of magnitude larger for the coating/substrate than for the base SS. The high resistance (R_p) values of the coatings are associated to non-open porosity, probably related to the

amorphous nature of the oxide film, but also to a certain effect of the components of the electrolyte. Figure 8 shows a rapid decrease in time of the R_p for the coating during the first hours of immersion (from 150 to 100 kΩ cm^2 during the first 100 hours) that illustrates some penetration within the confined nanoporous to the substrate.

Nevertheless, for longer immersion times, the R_p do not decrease any longer and a small recovery can be observed.

The R_p results are in agreement to the evolution of the total impedance as can be clearly observed in figure 9 where the value of the modulus of the impedance ($|Z|$) at 0.382 mHz are plotted as a function of the immersion time for both the SS and *a*-Nb_2O_5 samples. The impedance of the coatings is one order of magnitude larger than the steel and these values remain very stable during the length of the immersion experiments.

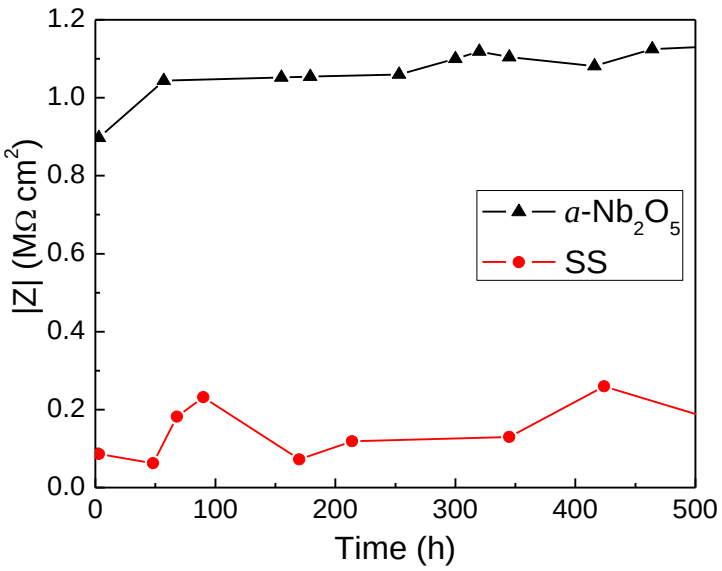

Figure 9. Modulus of the impedance value at the lowest frequency (0.382 mHz) as a function of the immersion time for both samples immersed in Hartman solution. KK analysis indicated that the measuremnts were reliable even at the low frequency range.

3.4 Ellipsometry

In order to elucidate if the different response of the niobium oxide films when immersed in the Hartman solution was related to the adsorption of the lactate on its surface, ellipsometry was used. Figure 10 shows the changes of the Δ ellipsometric angle (which is more sensitive to thickness variations) with time, for both the coating and substrate, as the immersion time increased up to 2400s. The change in Δ (δΔ) corresponds to the difference between the Δ values in Hartman and Δ values in NaCl (i. e., no organic molecule, which correspond to our baseline) for each surface.

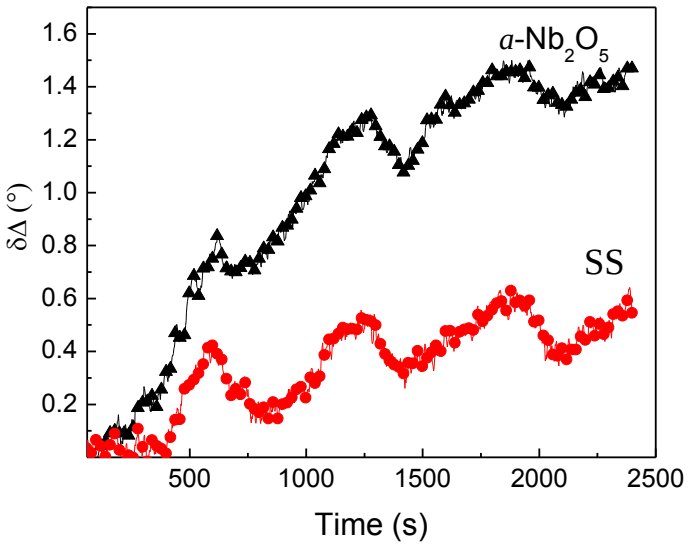

Figure 10. Kinetic ellipsomeric spectra showing the variation in Δ ellipsometer angle as the lactate from the Hartman solution is adsorbed on both sample's surfaces.

Figure 10 shows that the Δ variation is larger for the coating than for the substrate. The δΔ value obtained at the end of the experiment provides information about the adsorbed surface mass density (or thickness of the layer, or amount of protein adsorbed). It can be observed that the total change in Δ for the coating is larger than for the steel substrate, suggesting a larger surface mass density of the lactic acid. Therefore, qualitatively, the results in figure 10 indicated that there is more protein adsorbed in the a-Nb_2O_5 surface than in the steel substrate.

4. DISCUSSION

In this paper, the electrochemical response of amorphous niobium oxide thin films in two physiological solutions isotonic to the human blood was presented. The coating results were compared to the response from the stainless steel substrate. The coatings were deposited by reactive magnetron sputtering without heating the substrate and this lead to an amorphous dense oxide. The films were very thin (150 nm) and nevertheless, they showed current densities and potentials reduced in comparison to the substrate, especially when the Hartman solution was used. One clear result was the adhesive failure of the coating when immersed in the NaCl. Meanwhile, the electrochemical response of the coating in the Hartman solution indicated a stable and protecting coating. Adhesive failure of PVD coatings is usually related to the intrinsic nano-porosity associated to PVD coatings, which results from the growth mechanism.

One of the main disadvantages of the PVD coatings as protection barrier for corrosion is the presence of intrinsic micro or nanometric porosity. This porosity acts as an open path for the electrolyte to reach the substrate; this initiates a localized corrosion, which is highly aggressive for the stainless steel. Moreover, the attack occurring at the film-substrate interface leads to the loss of film

adhesion and in some cases catastrophic delamination occurs. This can be seen in figure 5, where extensive film delamination was observed for the *a*-Nb_2O_5/SS systems when a NaCl solution was used as the electrolyte. Surprisingly, this was not the case when the physiological solution containing lactic acid was used to study the electrochemical response of the coatings/SS systems. In the later case, the results showed that the *a*-Nb_2O_5 coating was stable for immersion times up to 500 hours; no strong variations in the modulus of the impedance or the phase angle were observed. This demonstrates high stability of the electrochemical system with no formation of active corrosion sites, either at the coating-electrolyte interface or the substrate-electrolyte interface, which can be reached through the small pores in the coating. The presence of any of these active corrosion sites would significantly lower the modulus of the impedance and the phase angle especially at the low frequency range. Moreover, there was a good agreement between the polarization resistance results and the corrosion current density of the *a*-Nb_2O_5 coating, indicating an improvement in the corrosion resistance of the coated-steel.

The difference between the response on NaCl and in the Hartman solution can be explained examining the ellipsometric results; there is a fast adsorption of the organic molecule on both surfaces, but the amount adsorbed on the coating is larger than on the steel. Moreover, the electrochemical stability observed for the coating in the Hartman solution, as opposite to the catastrophic effect observed in the NaCl, might be explained assuming that the lactic acid molecules block-out the porosity of the coatings. Therefore, there is synergetic effect which leads to the observed high corrosion resistance of the coatings in Hartman; this may also explain the more negative phase angle showed for the samples after 155 hours of immersion, i. e. after completed blocking of the pores has occurred. The lactate molecule is able to cover the surface and also penetrate into the pores due to its small size, about 0.5 nm along the larger axis impeding the pass of the electrolyte. A similar phenomenon was proposed by Assis et al.[14] to explain the corrosion behavior of a Ti-Nb alloy when immersed in three different physiological simulated fluids, the adsorption and penetration into the porous oxide layer of the organic molecules was confirmed by surface analysis. The adsorption of organic molecules on metal oxides can occur by chemisorption or physisorption, and once they are adsorbed they can interact to form precipitates as well as ternary surface complexes with cations, giving an absorbed passive layer, which will also enhanced the corrosion resistance of the material.

The contradiction between the catastrophic fail of the films when immersed in pure NaCl solutions and the good resistance presented in the Hartman solution shows the importance of evaluating the materials in appropriate electrolytes [15].

5. CONCLUSIONS

Amorphous niobium oxide films deposited on stainless steel substrates were produced by magnetron sputtering to evaluate the corrosion resistance provided by the coating when immersed in simulated physiological fluids. The results obtained in this work suggested that the adsorption of small organic molecules on the surface of the *a*-Nb2O5 forms a passive layer, which blocks-out the intrinsic porosity of the coatings, leading to large impedance values of the coatings even after large immersion

times. The EIS analysis showed that the polarization resistance of the coatings was one order of magnitude larger than the SS, and therefore the corrosion rate of coated-SS should be significantly reduced. Note that even with such good behavior in Hartman, we cannot conclude that the coating is a good candidate for corrosion protection of biomedical implants, analysis using more complex electrolytes or electrolytes containing larger organic molecules or concentrations should be done before reaching any conclusion. However, a relevant result from this research was to establish the large differences in the corrosion behavior of the surfaces depending on the medium composition, striking the importance of in-vitro testing biomaterials using electrolytes that really simulated the functional environment for a particular application.

ACKNOWLEDGEMENTS
Financial support from DGAPA-PAPIIT projects IN102907-IN103910 and CONACYT P45833 is gratefully acknowledged. P.N. Rojas acknowledges to the CONACYT for a PhD scholarship. Special thanks to the technicians O. Novelo and H. Zarco.

References

1. A. Balamurugan, S. Rajeswari, G. Balossier, A. H. S. Rebelo, and J. M. F. Ferreira, *Materials and Corrosion-Werkstoffe Und Korrosion* 59, 855-869 (2008).
2. M. Sivakumar, U. K. Mudali, and S. Rajeswari, *Steel Res* 65, 76-79 (1994).
3. M. A. Malik, P. J. Kulesza, and G. Pawlowska, *Electrochimica Acta* 54, 5537-5543 (2009
4. M. T. Duffy, Zaininge.Kh, and C. C. Wang, *Journal of the Electrochemical Society* 115, (1968).
5. A. Shahryari, S. Omanovic, and J. A. Szpunar, *Materials Science & Engineering C-Biomimetic and Supramolecular Systems* 28, 94-106 (2008).
6. M. Fenker, M. Balzer, H. Kappl, and O. Banakh, *Surface & Coatings Technology* 200, 227-231 (2005).
7. E. Eisenbarth, D. Velten, M. Müller, R. Thull, and J. Breme, *Journal of Biomedical Materials Research Part* A 79A, 166-175 (2006).
8. G. Ramirez, S. E. Rodil, S. Muhl, D. Turcio-Ortega, J. J. Olaya, M. Rivera, E. Camps, and L. Escobar-Alarcon, *Journal of Non-Crystalline Solids* 356, 2714-2721 (2010).
9. C. Liu, Q. Bi, A. Leyland, and A. Matthews, *Corrosion Science* 45, 1243-1256 (2003).
10. E. J. Giordano, N. Alonso-Falleiros, I. Ferreira, and O. Balancin, *Rem-Revista Escola De Minas* 63, 159-166 (2010).
11. C. Liu, Q. Bi, A. Leyland, and A. Matthews, *Corrosion Science* 45, 1257-1273 (2003).
12. P. A. Cuypers, J. W. Corsel, G. M. Willems, and W. T. Hermens, *Abstr Pap Am Chem* S 192, 32-Coll (1986).
13. B. Tutunaru, A. Patru, I. Bibicu, and M. Preda, *J Optoelectron Adv* M 9, 3400-3404 (2007).
14. S. L. Assis, S. Wolynec, and I. Costa, *Materials and Corrosion-Werkstoffe Und Korrosion* 59, 739-743 (2008).
15. S. Virtanen, I. Milosev, E. Gomez-Barrena, R. Trebse, J. Salo, and Y. T. Konttinen, *Acta Biomaterialia* 4, 468-476 (2008).